

# Automatic Tracking of Surgical Instruments with A Continuum Laparoscope Using Data-driven Control in Robotic Surgery

Xiaowen Kong<sup>1</sup>, Hangjie Mo<sup>1</sup>, Erbao Dong<sup>1</sup>, Yunhui Liu<sup>1</sup>, and Dong Sun<sup>1</sup>

<sup>1</sup>Affiliation not available

July 6, 2022

## Abstract

In existing surgery process, surgeons need to manually adjust the laparoscopes to provide a better field of view during operation, which may distract surgeons and slow down the surgery process. This paper presents a data-driven control method that uses a continuum laparoscope to adjust the field of view by tracking the surgical instruments. A Koopman-based system identification method is firstly applied to linearize the nonlinear system. Shifted Chebyshev polynomials are used to construct observation functions that transfer low-dimension observations to high-dimension ones. The Koopman operator is approximated using a finite-dimensional estimation method. An optimal controller is further developed according to the trained linear model. Furthermore, a learning-based pose estimation framework is designed to detect keypoints on surgical instruments and provide visual feedback for adjusting the laparoscope. Compared with other detection methods, the proposed scheme achieves a higher detection precision and provides more optional keypoints for tracking. Simulation and experiments validate the feasibility of the proposed control method. Experiment results show that the proposed method can automatically adjust the field of continuum laparoscope through tracking surgical instruments in a timely manner and the number of surgical tools is not limited.

## ToC Figure

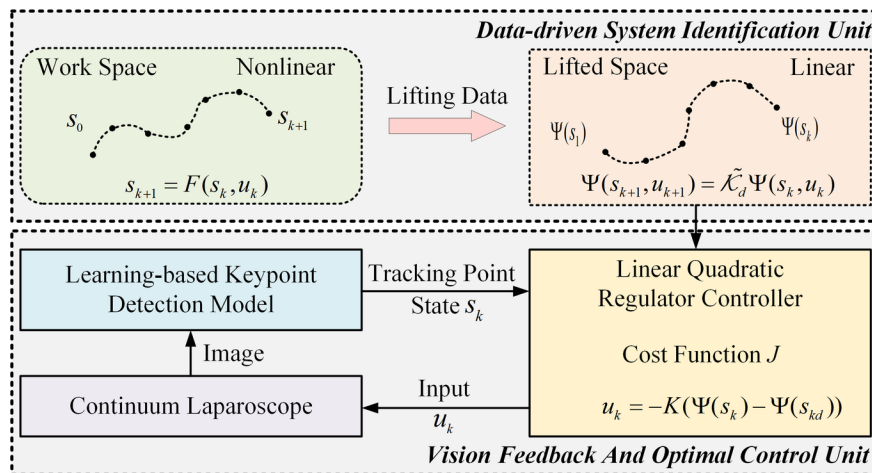


Figure 1: Framework of the automatic tracking system of the surgical instruments with a continuum laparoscope. This is a caption

# Introduction

Robot-assisted minimally invasive surgery (RMIS) has received an increasing amount of attention because of its unique advantages compared with traditional open surgery.<sup>[1-5]</sup> In RMIS, laparoscopes used to display the surgical scenario on a screen are usually held by a robotic arm instead of an assistant. Surgeons need to frequently pause the operation of surgical instruments and adjust the laparoscope to provide a better field of view (FOV). This distracts the surgeon during the surgery, thereby prolonging the operation time and causing surgeon fatigue.

A laparoscopic control method to adjust the FOV of laparoscopy by tracking surgical instruments automatically during the surgical procedure needs to be developed. Currently, rigid laparoscopy is widely applied to RMIS with automatic FOV adjusting algorithms. Yang et al. proposed a region-based visual servoing method to automatically manipulate laparoscopy with colored markers, which can improve the control efficiency and safety of FOV.<sup>[6]</sup> An autonomous surgical instrument tracking method without any markers was further proposed based on the visual tracking space vector.<sup>[7]</sup> However, these methods encounter the workspace problem. When operating a rigid laparoscopy using a robotic arm, avoiding collision between the robot arm and the other surgical instruments is necessary. Therefore, using a robotic arm to operate a rigid laparoscope in a narrow workspace is difficult, leading to the limited adjustment workspace of rigid laparoscopy.

Continuum manipulators have been widely applied in robotic surgical applications due to their higher dexterity and less workspace required.<sup>[8-10]</sup> Recently, continuum manipulators have been used for automatic FOV adjustment with visual servoing in RMIS.<sup>[11]</sup> However, the dynamics of continuum manipulator are always highly nonlinear and high-dimensional due to the mechanical compliance of its structure.<sup>[12]</sup> These characteristics bring challenges to the precise control of continuum manipulators. Existing methods usually simplify the continuum manipulator based on physical assumptions in establishing dynamic models, such as piecewise constant curvature model, pseudo-rigid-body, quasistatic and simplified geometry.<sup>[13-20]</sup> Assumptions in these simplified models may lead to deviation under actual conditions and inaccurate results, which are not feasible for use in practice, especially for scenarios with high precision requirements.

Recently, data-driven control methods such as neural networks and reinforcement learning, have shown great potential for controlling continuum manipulators.<sup>[21,22]</sup> The advantage of these methods lies in the input-output mapping of the system derived from sensing data without analytical modelling and complex computation. Given enough collected input-output data, data-driven models can describe the behavior of the system over its entire operating range. However, these methods usually require many tuning parameters and repeated trials to establish accurate models. Other concerns include low real-time performance and computational complexity.<sup>[23]</sup> Koopman operator provides an alternative solution for establishing the dynamic model of a continuum manipulator based on its unique linear structure.<sup>[24,25]</sup> Koopman operator lifts the nonlinear dynamic model of the system into an infinite-dimensional space and evolves the state functions, which are also called observation functions in the new space. In this way, the dynamic model of the nonlinear system can be easily propagated in a linear manner, relying on input-output data only. As a result, linear control methods can be applied to control the continuum manipulator with high precision.

Apart from accurate system identification, a close-loop control with high precision visual feedback is also important. Visual feedback in laparoscopic instruments tracking can be divided into two types: marked methods and unmarked methods. Marked methods manually add a characteristic marker on the instrument for easy detection. Although this method can localize the target quickly, uncertainty exists due to the presence of blood and gas during surgery. Furthermore, this method provides surgeons with a poor experience and has a low tracking precision because markers are usually located at a non-client rod of the instrument. Unmarked methods usually choose the whole metal part of the instrument as the detecting area and then detect the area as an object detection task using a deep learning algorithm.<sup>[26]</sup> However, this method requires surgeons to focus on different points of operation at different stages of surgery, and the method is often not flexible enough. For example, the ultrasonic knife in surgery used to resect tissue and the focused point should be

the tip of the instrument. Scissors are used to clamp tissues or needles, so the focused point should be the center of the clasper. Therefore, the unmarked methods result in a less accurate visual feedback.

In this present work, we focus on autonomous control of a continuum laparoscope to adjust the FOV and keep the surgical instruments at the view center in RMIS. To address this critical issue, we proposed an automatic surgical instrument tracking framework based on a Koopman-based control scheme and learning-based vision feedback. This framework can be divided into two units. The first unit is the data-driven system identification unit, which applies the Koopman operator to transfer a nonlinear dynamics system into a linear closed-loop control. Unlike the Taylor-based method, we introduce the Chebyshev polynomials to choose observation functions.<sup>[27,28]</sup> Chebyshev polynomials is a global approximation method dependent on high-order derivatives of the system state as existing methods. The approximation error of the proposed method is also analyzed. A linear quadratic regulator (LQR) controller is further used for real-time control based on the linear representation of the continuum laparoscope.

The second unit is the visual feedback and optimal control unit, which provides control feedback for the surgical instruments tracking task. In this unit, a deep keypoints detection network is developed to predict the pixel positions of keypoints on the surgical instruments. Unlike the existing object detection methods, a pose estimation method is developed to detect the keypoints on surgical instruments. The pose estimation method can directly regress the pixel coordinates of the keypoints on surgical instruments, instead of detecting the whole area as the object detection method. This method can increase the precision of keypoints detection, and is beneficial to the subsequent control tasks. The keypoints needed as the tracking point can be selected flexibly according to different surgery stages in the following control system. In addition, weights of different surgical instruments can be set by surgeons when multiple instruments are used according to their requirements.

## Experimental Section/Methods

We build an experiment platform based on the proposed automatic tracking system to validate the data-driven control method. A 2mm diameter pinhole camera with a resolution of  $400 \times 400$  pixels is fixed at the end effector of the cable-driven continuum manipulator (Intuitive Surgical, California, USA). Sensing image can be obtained with a frequency of 30 Hz through a USB port. The continuum manipulator has four connected joints, which can be divided into two groups. Joint1 and Joint4 control movement in the X-axis direction, and both are actuated by a brushless motor (Maxon Group, Sachseln, Switzerland). Joint2 and Joint3 control movement in the Y-axis direction and are actuated by another brushless motor. The continuum manipulator is fixed in the Z-axis direction, which could ensure safety once the initial position is determined. Elmo drivers (Elmo Motion Control Ltd., Israel) are used to actuate motors precisely by receiving command from TwinCAT3 (Beckhoff Automation GmbH & Co. KG, Germany) through the EtherCAT bus. The Large Needle Driver and the Grasping Retractor (Intuitive Surgical, California, USA) are used in this work.[4] The Large Needle Driver holds the needle while forcing the tip through the tissue to complete the suturing task in RMIS. Grasping Retractor are used to retract the tissue to reveal the surgical scope so that the surgeon can explore the surgical area and perform surgery.

In order to calculate the infinite-dimensional approximation of the Koopman Operator, a set of system states and corresponding inputs were collected. We collected 100 trials with random initial inputs of the motors. Then the input of the two motors varies one cycle according to the trigonometric function to generate the states. Following this rule, the continuum laparoscope runs 500 steps a cycle in the workspace. Finally, we collected 50,000 pairs of data about system states and inputs. The Koopman operator of the continuum laparoscope system is estimated according to the system identification method.

Furthermore, we also evaluate the dynamic uncertainty of the continuum laparoscope system based on the data collection. Dynamical uncertainty means that the same inputs may lead to slightly different outputs.

This uncertainty is caused by motor encoder error and system assembly error. Specifically, the system gets input that changes periodically.

The output of the system over 100 cycles is then collected, and the standard error over 100 cycles is calculated. The standard error of the system is 19 pixels. The internal error of this system will affect our tracking experiment, which cannot be eliminated by the designed controller.

## Results

### Experiments on tracking static instruments

To evaluate the autonomous laparoscopic control method to adjust the view of a continuum laparoscope, we perform the experiments on static surgical instruments. We conduct repeat trials for different surgical instruments. Only the initial position of the surgical instrument is different. As shown in Figure 2(a), the black point represents the initial position of the tracking keypoint on the surgical instrument. The scatters mean the position of the tracking point relative to the center of the FOV at each step. Figure 2(b) shows the distance between the tracking point and the FOV center of the laparoscope. When the continuum laparoscopy was controlled to automatically adjust the FOV based on visual feedback, it needs approximately 25 steps to approach the center of the FOV. This is consistent with our verification in the simulation environment. After 25 steps, the continuum laparoscope remains largely stationary, indicating that our approach provides a stable FOV after the tracking purpose is reached. The tracking error is approximately 39.1 pixels when the system is stable.

Figure 2(c) shows the keypoints on the two surgical instruments and the pixel position of our tracking points relative to the center of the FOV at each step. Notably, the weights of both surgical instruments in the FOV are the same. Figure 2(d) shows changes of the tracking error and relative position of the two surgical instruments, which is consistent with the performance when a single surgical instrument tracking task is performed. The performance of tracking static surgical instruments proves the feasibility of our proposed data-driven control approach.

### Experiments on tracking moving instruments

Firstly, we evaluate the proposed method with one moving surgical instrument. As shown in Figure 3(a), the scatters represent the relative position of the tracking points on the surgical instrument in the FOV of the continuum laparoscope. The number of color-bar means the density of the tracking points in the image plane. The higher the value, the more times the tracking point locates in the area with the movement of surgical instrument. It is seen that most of the tracking points locate near the center of the FOV. The distance between the tracking point and FOV center of the laparoscope is shown in Figure 3(b). The average distance while tracking a moving surgical instrument is approximately 45.77 pixels.

Secondly, we extend the tracking task to two surgical instruments. We set the same weights for the two surgical instruments in the tracking process. The same weights mean the tracking point is located at the midpoint of the keypoint on the two surgical instruments. Figure 3(c) shows the relative pixel position of the tracking points in the image plane. Figure 3(d) shows tracking error while tracking double surgical instruments. The average distance is about 28.47 pixels.

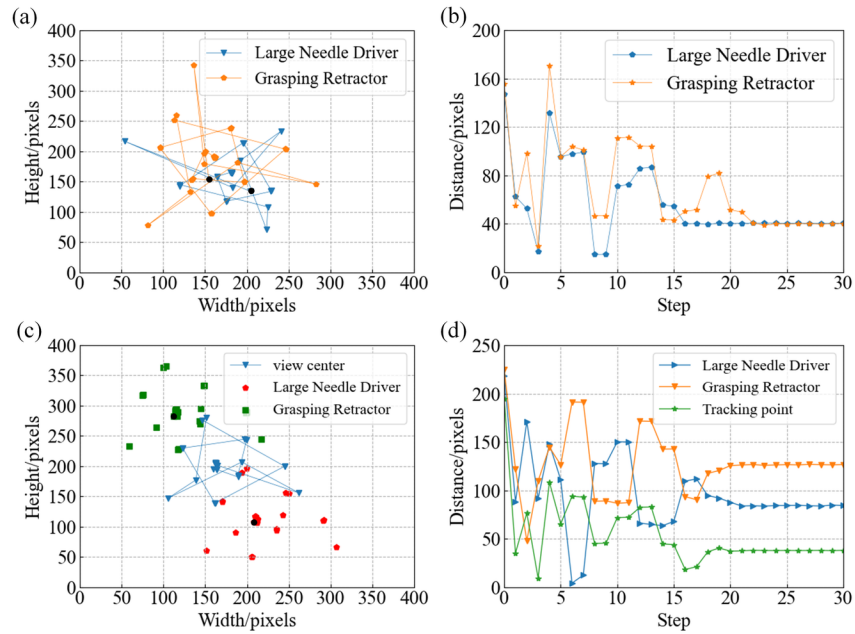


Figure 2: Experimental results while the continuum laparoscope tracking the static instruments (Large Needle Driver and Grasping Retractor). Black points mean the initial position of tracking point in FOV. (a) Tracking the two surgical instruments respectively with different initial position. (b) Distances between the tracking point and the center of FOV while tracking the two surgical instruments respectively. (c) Tracking the two surgical instruments simultaneously. (d) Distances between the tracking point (center of the two instruments) and the center of FOV.

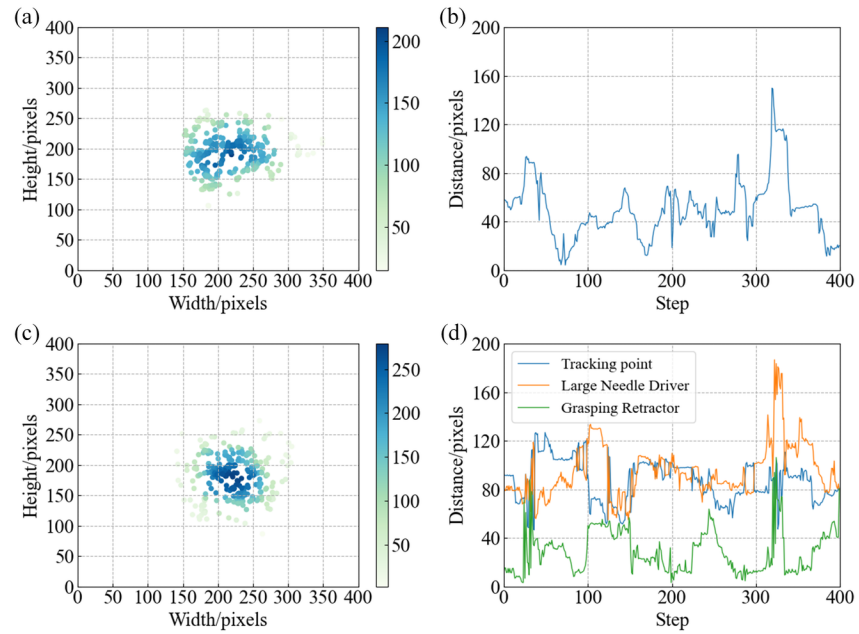


Figure 3: Pixel position of the moving surgical instruments (Large Needle Driver and Grasping Retractor) compared with initial position. Color bar represents the position density. (a) Pixel coordinates density of the tracking point while the single surgical instrument moving. (b) Distances between the target position and center of the view while tracking the single surgical instrument. (c) Pixel coordinates density of the tracking point while the double surgical instrument moving simultaneously. (d) Distances between the target position (center of the two instruments) and center of the view.

## Discussion

Researchers reported the clinical requirements for adjusting the FOV of the laparoscope with the movement of surgical instruments.<sup>[7]</sup> The researchers analyzed collected videos of different clinical surgeries. They found that the average distance from the tip of the surgical instruments to the FOV center of the laparoscope was about 423.84 pixels, even though the surgical assistant was constantly adjusting the laparoscopic field of vision during the procedure. Considering the resolution of collected surgical videos, the error is approximately 22.08% of the horizontal resolution and 39.24% of the vertical resolution.

We have demonstrated the feasibility of our proposed autonomous laparoscopic control approach to adjust FOV regardless of whether the surgical instruments are moving. Although the fast movement of surgical instruments leads to the accuracy of keypoint detection and then affects the accuracy of surgical instrument tracking. From the experiment results on the automatic tracking task of surgical instruments, the distances between the tracking point and the center of FOV while tracking single moving instruments and double moving instruments are about 45.77 pixels and 28.47 pixels, respectively. The results are approximately 11.44% and 7.12% of our continuum laparoscopic FOV, which is also much smaller than the FOV error of clinical surgery. Considering the dynamic uncertainty of the continuum laparoscope system, the internal error of this system is about 19 pixels. This indicates our autonomous FOV adjusting method with a continuum laparoscope can satisfy the clinical requirements. In addition, laparoscopic FOV adjustment as part of the surgical procedure, our approach can promote the automation of the robotic surgery process.

## Conclusion

This article presents a data-driven control method for a continuum laparoscope system with learning-based visual feedback to adjust the FOV automatically in RMIS. We first develop a nonlinear system identification method using the Koopman operator and Chebyshev polynomials. Then we build an LQR controller based on the trained Koopman Operator with the visual feedback. To provide precise visual feedback for the control system, a learning-based keypoint detection method is designed without any manual markers. This method provides more options for selecting keypoints on surgical instruments during the different surgical processes while ensuring detecting accuracy. Simulation and experiments are performed to evaluate the proposed methods. Compared with other keypoint detection methods, the pose estimation method provides higher accuracy. Tracking experiments show the feasibility of the proposed data-driven control method of a continuum laparoscope for adjusting the FOV automatically. Experiments results shows that the proposed method can also satisfy the clinical requirements. In the future, the freedom of continuum laparoscope in Z-axis direction to enlarge the view will be considered to provide surgeons a better experience. Constrained workspaces and inputs will be studied to ensure safety during robotic surgery.

## Acknowledgements

Xiaowen Kong and Hangjie Mo contributed equally to this work. This work was supported by the Research Grants Council of the Hong Kong Special Administrative Region, China (Ref. no. T42-409/18R and no.11211421).

## Conflict of interest

The authors declare no conflict of interest.

## References

- [1] M. Thai, P. Phan, T. Hoang, S. Wong, N. Lovell, T. Do, Advanced intelligent systems for surgical robotics. *Adv. Intell. Syst.* **2020**, *2*, 1900138.
- [2] C. Gao, H. Phalen, S. Sefati, J. Ma, R. Taylor, M. Unberath, M. Armand, Fluoroscopic navigation for a surgical robotic system including a continuum manipulator. *IEEE Trans. Biomed. Eng.* **2022**, *69*, 453.
- [3] Y. Huang, J. Li, X. Zhang, K. Xie, J. Li, Y. Liu, C. Ng, P. Chiu, Z. Li, A surgeon preference-guided autonomous instrument tracking method with a robotic flexible endoscope based on dVRK platform. *IEEE Robot. Autom. Lett.* **2022**, *7*, 2250.
- [4] X. Kong, Y. Jin, D. Qi, Z. Wang, Z. Rui, B. Lu, E. Dong, Y. Liu, D. Sun, Accurate instance segmentation of surgical instruments in robotic surgery: model refinement and cross-dataset evaluation. *Int. J. Comput. Assist. Radiol. Surg.* **2021**, *16*, 1607.
- [5] P. Dupont, B. Nelson, M. Goldfarb, B. Hannaford, A. Menciassi, M. O'Malley, N. Simaan, P. Valdastri, G. Yang, A decade retrospective of medical robotics research from 2010 to 2020. *Sci. Robot.* **2021**, *6*, eabi8017.
- [6] B. Yang, W. Chen, Z. Wang, Y. Lu, J. Mao, H. Wang, Y. Liu, Adaptive FOV control of laparoscopes with programmable composed constraints. *IEEE Trans. Med. Robot. Bionics* **2019**, *1*, 206.
- [7] L. Li, X. Li, B. Ouyang, S. Ding, S. Yang, Y. Qu, Autonomous multiple instruments tracking for robot-assisted laparoscopic surgery with visual tracking space vector method. *IEEE/ASME Trans. Mech.* **2022**, *27*, 733.
- [8] W. Zeng, J. Yan, K. Yan, X. Huang, X. Wang, S. Cheng, Modeling a symmetrically-notched continuum neurosurgical robot with non-constant curvature and superelastic property. *IEEE Robot. Autom. Lett.* **2021**, *6*, 6489.
- [9] H. Mo, R. Wei, B. Ouyang, L. Xing, Y. Shan, Y. Liu, D. Sun, Control of a flexible continuum manipulator for laser beam steering. *IEEE Robot. Autom. Lett.* **2021**, *6*, 1074.
- [10] J. Wang, A. Chortos, Control Strategies for Soft Robot Systems. *Adv. Intell. Syst.* **2022**, *4*, 2100165.
- [11] F. Anooshahpour, P. Yadmellat, I. Polushin, R. Patel, A motion transmission model for a class of tendon-based mechanisms with application to position tracking of the da Vinci instrument. *IEEE/ASME Trans. Mech.* **2019**, *24*, 538.
- [12] X. Huang, J. Zou, G. Gu, Kinematic modeling and control of variable curvature soft continuum robots. *IEEE/ASME Trans. Mech.* **2021**, *26*, 3175.

- [13] D. Bruder, X. Fu, R. Gillespie, C. Remy and R. Vasudevan, Data-driven control of soft robots using Koopman operator theory, *IEEE Trans. Robot.* **2021**, *37*, 948.
- [14] R. Webster, B. Jones, Design and kinematic modeling of constant curvature continuum robots: a review. *Int. J. Robot. Res.* **2010**, *29*, 1661.
- [15] K. Nuelle, T. Sterneck, S. Lilge, D. Xiong, J. Burgner-Kahrs, T. Ortmaier, Modeling, calibration, and evaluation of a tendon-actuated planar parallel continuum robot. *IEEE Robot. Autom. Lett.* **2020**, *5*, 5811.
- [16] S. Huang, D. Meng, X. Wang, B. Liang, W. Lu, A 3D static modeling method and experimental verification of continuum robots based on pseudo-rigid body theory. *Proc. IEEE/RSJ Int. Conf. Rob. Syst. (IROS)* **2019**, 4672
- [17] D. Bruder, A. Sedal, R. Vasudevan, C. Remy, Force generation by parallel combinations of fiber-reinforced fluid-driven actuators. *IEEE Robot. Autom. Lett.* **2018**, *3*, 3999.
- [18] T. Thuruthel, E. Falotico, F. Renda, C. Laschi, Model-based reinforcement learning for closed-loop dynamic control of soft robotic manipulators. *IEEE Trans. Robot.* **2019**, *35*, 124.
- [19] A. Sedal, A. Wineman, R. Gillespie and C. Remy, Comparison and experimental validation of predictive models for soft, fiber-reinforced actuators. *Int. J. Robot. Res.* **2021**, *40*, 119.
- [20] D. Bruder, A. Sedal, J. Bishop-Moser, S. Kota, R. Vasudevan, Model based control of fiber reinforced elastofluidic enclosures. *Proc. IEEE Int. Conf. Robot. Autom. (ICRA)* **2017**, 5539.
- [21] K. Chin, T. Hellebrekers, C. Majidi, Machine Learning for Soft Robotic Sensing and Control. *Adv. Intell. Syst.* **2020**, *2*, 1900171.
- [22] G. Mamakoukas, M. Castaño, X. Tan, T. D. Murphey, Derivative-based koopman operators for real-time control of robotic systems. *IEEE Trans. Robot.* **2021**, *37*, 2173.
- [23] I. Abraham, T. D. Murphey, Active learning of dynamics for data-driven control using Koopman operators. *IEEE Trans. Robot.* **2019**, 351071-1083.
- [24] D. Bruder, C. Remy, R. Vasudevan, Nonlinear system identification of soft robot dynamics using Koopman operator theory. *Proc. IEEE Int. Conf. Robot. Autom. (ICRA)* **2019**, 6244.
- [25] M. Korda, I. Mezić, Linear predictors for nonlinear dynamical systems: Koopman operator meets model predictive control. *Automatica* **2018**, *93*, 149.
- [26] B. Li, B. Lu, Y. Lu, Q. Dou, Y. Liu, Data-driven holistic framework for automated laparoscope optimal view control with learning-based depth perception. *Proc. IEEE Int. Conf. Robot. Autom. (ICRA)* **2021**, 12366.
- [27] D. Shuman, P. Vandergheynst, D. Kressner, P. Frossard, Distributed signal processing via chebyshev polynomial approximation. *IEEE. Trans. Signal Inf. Process Netw.* **2018**, *4*, 736.
- [28] L. Wang, Y. Chen, D. Liu, D. Boutat, Numerical algorithm to solve generalized fractional pantograph equations with variable coefficients based on shifted Chebyshev polynomials. *Int. J. Comput. Math.* **2019**, *96*, 2487.
- [29] M. Williams, I. Kevrekidis, C. Rowley, A data-driven approximation of the Koopman operator: extending dynamic mode decomposition. *J. Nonlinear Sci.* **2015**, *25*, 1307.
- [30] T. Çimen, State-dependent Riccati equation (SDRE) control: a survey. *IFAC Proc. Vol.* **2008**, *41*, 3761.
- [31] A. Ahmadian, S. Salahshour, C. Chan, Fractional differential systems: a fuzzy solution based on operational matrix of shifted Chebyshev Polynomials and its applications. *IEEE Trans Fuzzy Syst.* **2017**, *25*, 218.

- [32] X. Du, T. Kurmann, P. Chang, M. Allan, S. Ourselin, R. Sznitman, J. Kelly, D. Stoyanov, Articulated multi-instrument 2-D pose estimation using fully convolutional networks. *IEEE Trans. Med. Imaging.* **2018**, 37, 1276.
- [33] Z. Luo, Z. Wang, Y. Huang, L. Wang, T. Tan, E. Zhou, Rethinking the heatmap regression for bottom-up human pose estimation. *Proc. IEEE/CVF Conf. Comput. Vis. Pattern Recog. (CVPR)* **2021**, 13264.
- [34] L. Sharan, G. Romano, J. Brand, H. Kelm, M. Karck, R. Simone, S. Engelhardt, Point detection through multi-instance deep heatmap regression for sutures in endoscopy. *Int. J. Comput. Assist. Radiol. Surg.* **2021**, 16, 2107.
- [35] B. Cheng, B. Xiao, J. Wang, H. Shi, T. Huang, L. Zhang, Higherhrnet: scale-aware representation learning for bottom-up human pose estimation. *Proc. IEEE/CVF Conf. Comput. Vis. Pattern Recog. (CVPR)* **2020**, 5386.
- [36] C. Payer, D. Štern, H. Bischof, M. Urschler, Integrating spatial configuration into heatmap regression based CNNs for landmark localization. *Med. Image Anal.* **2019**, 54, 207.
- [37] K. Han, Y. Wang, Q. Tian, J. Guo, C. Xu, C. Xu, Ghostnet: more features from cheap operations. *Proc. IEEE/CVF Conf. Comput. Vis. Pattern Recog. (CVPR)* **2020**, 1580.
- [38] S. Woo, J. Park, J. Lee, I. Kweon, Cbam: convolutional block attention module. *Proc. Europ. Conf. on Comput. Vis. (ECCV)* **2018**, 3.
- [39] S. Liu, L. Qi, H. Qin, J. Shi, J. Jia, Path aggregation network for instance segmentation. *Proc. IEEE/CVF Conf. Comput. Vis. Pattern Recog. (CVPR)* **2018**, 8759.
- [40] N. Ma, X. Zhang, M. Liu, J. Sun, Activate or not: Learning customized activation. *Proc. IEEE/CVF Conf. Comput. Vis. Pattern Recog. (CVPR)* **2021**, 8032.
- [41] E. Todorov, T. Erez, Y. Tassa, MuJoCo: A physics engine for model-based control. *Proc. IEEE/RSJ Int. Conf. Rob. Syst. (IROS)* **2012**, 5026.